Supporting Information

Surface composition and structural changes on titanium oxide-supported AuPd nanoparticles during CO oxidation

Angela A. Teixeira-Neto,[a] Renato V. Gonçalves,[b,c] Cristiane B. Rodella,[d] Liane M. Rossi,[b] Erico Teixeira-Neto[a]*

[a] Electron Microscopy Laboratory, LNNano-CNPEM, P.O. box 6192, 13083-970, Campinas, SP, Brazil.

[b] Lab. Nanomaterials & Catalysis, Institute of Chemistry-USP, P.O. box 26077, 05513-970, São Paulo, SP, Brazil.

[c] São Carlos Institute of Physics, University of São Paulo, PO Box 369, 13560-970, São Carlos, SP, Brazil.

[d] Brazilian Synchrotron Light Lab., LNLS-CNPEM, P.O. box 6192, 13083-970, Campinas, SP, Brazil.

E-mail: erico.neto@lnnano.cnpem.br.

XPS Spectra

Data mining for determination of the catalyst surface composition from raw XPS spectra was performed using Thermo Avantage Software©. Smart Background subtraction method was applied to the raw XPS spectra. This method is based on the Shirley[1] background function with the additional constraint that the background should not be of a greater intensity than the actual data at any point in the energy range. Peaks corresponding to constituent elements were deconvoluted using a Gaussian-Lorentzian product function and integrated at their full widths at half maximum (FWHM) for quantification. For the case of Pd quantification, a peak corresponding to Au4d orbitals is within the energy range of Pd3d, in the deconvoluted peaks shown in Figure S1a. The $Au4d_{5/2}$ contribution is simply subtracted from the raw spectrum (Figure S1b) and the Pd3d data may be integrated reliably. The result of this data mining procedure is shown in Figure S2, for all catalysts investigated in this work. Au 4f spectra of oxidized and reduces samples are presented in Figure S3.

1 - D.A. Shirley, *Phys. Rev. B* **1972**, 5**,** 4709–4714.

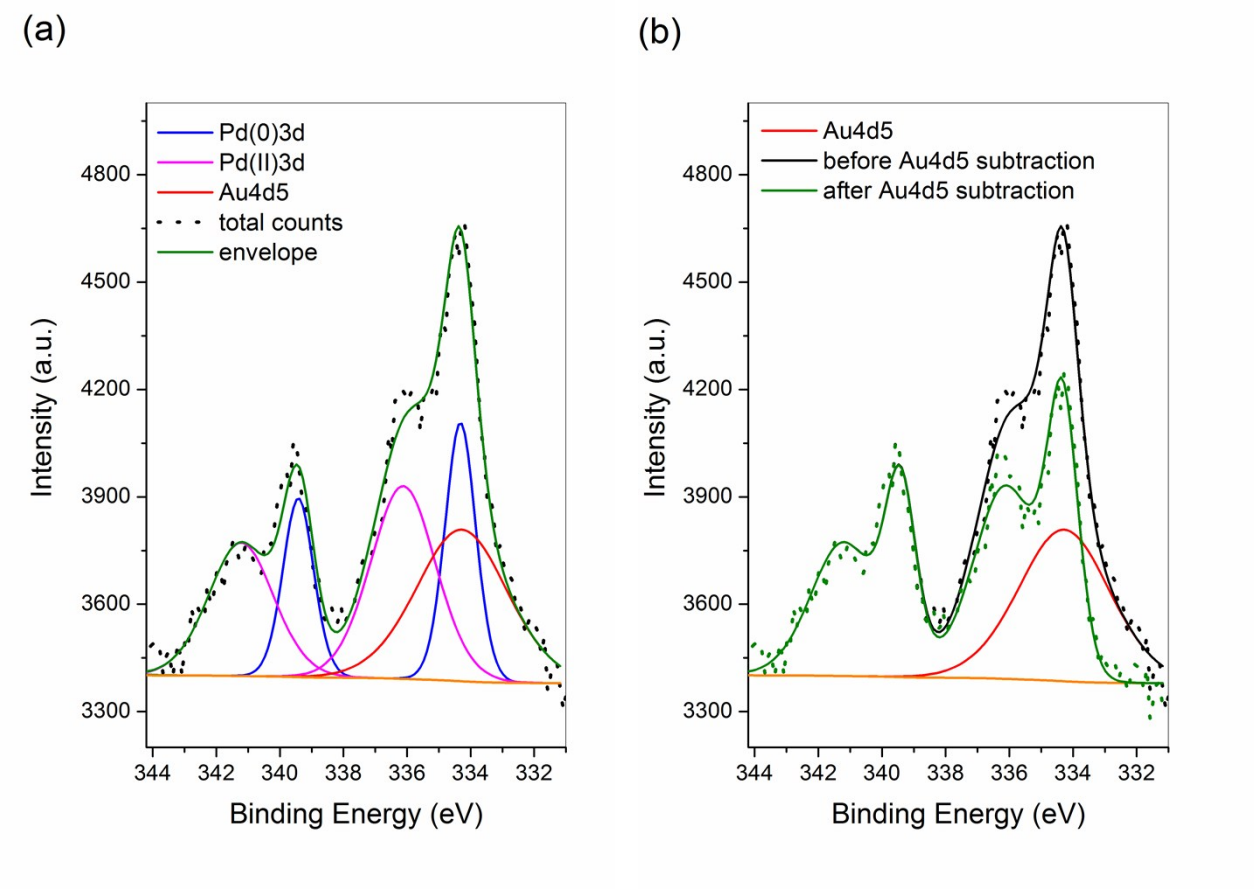

Figure S1. Example of the data mining procedure employed on X-ray photoelectron spectra of an reduced AuPd/TiO_2 material in the Pd3d region: (a) original count curve and deconvoluted peaks and (b) effect of the subtraction of $Au4d_{5/2}$ component.

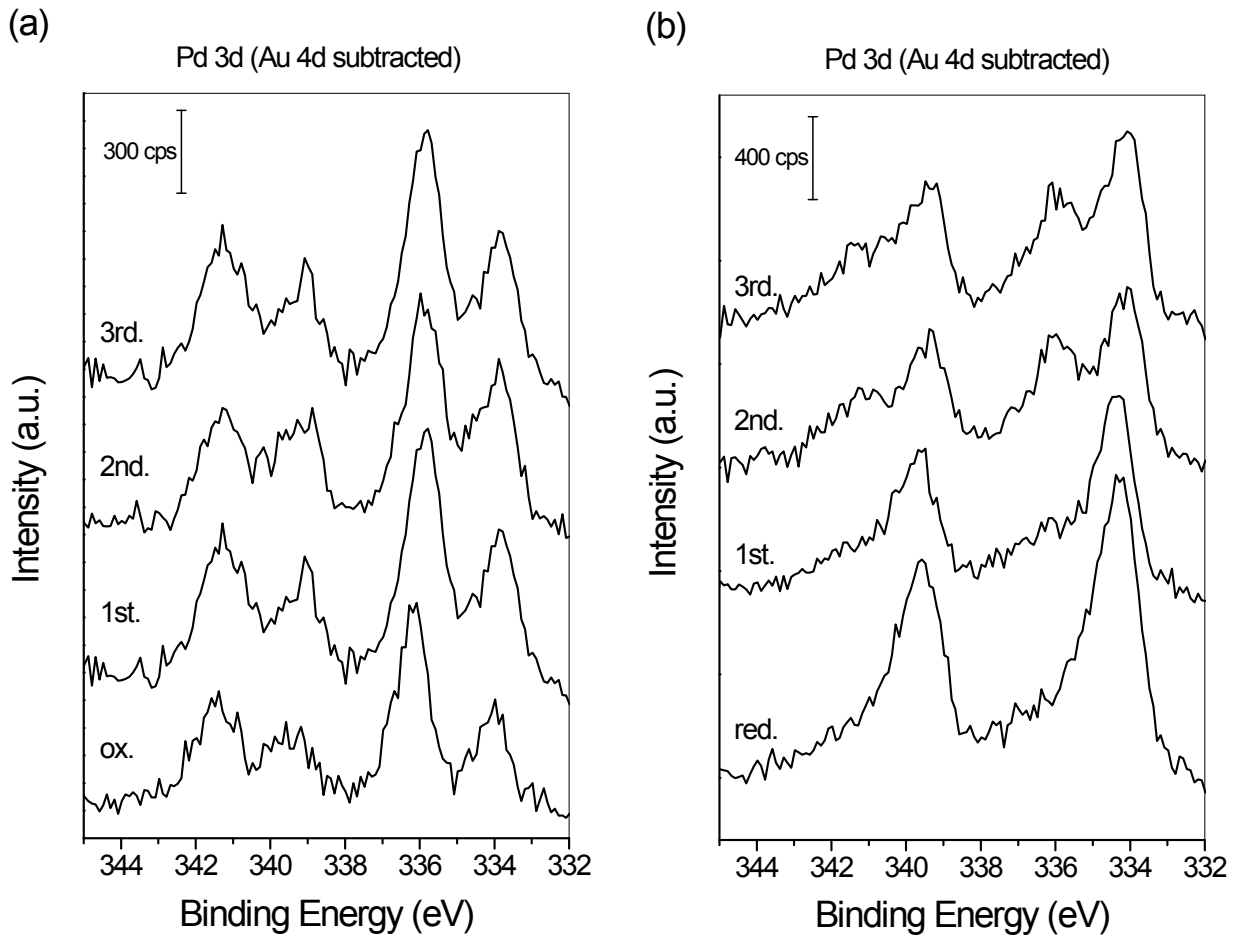

Figure S2. X-ray photoelectron spectra of the AuPd/TiO_2 materials in the Pd3d region measured after the indicated CO oxidation temperature ramps: (a) oxidized samples and (b) reduced samples.

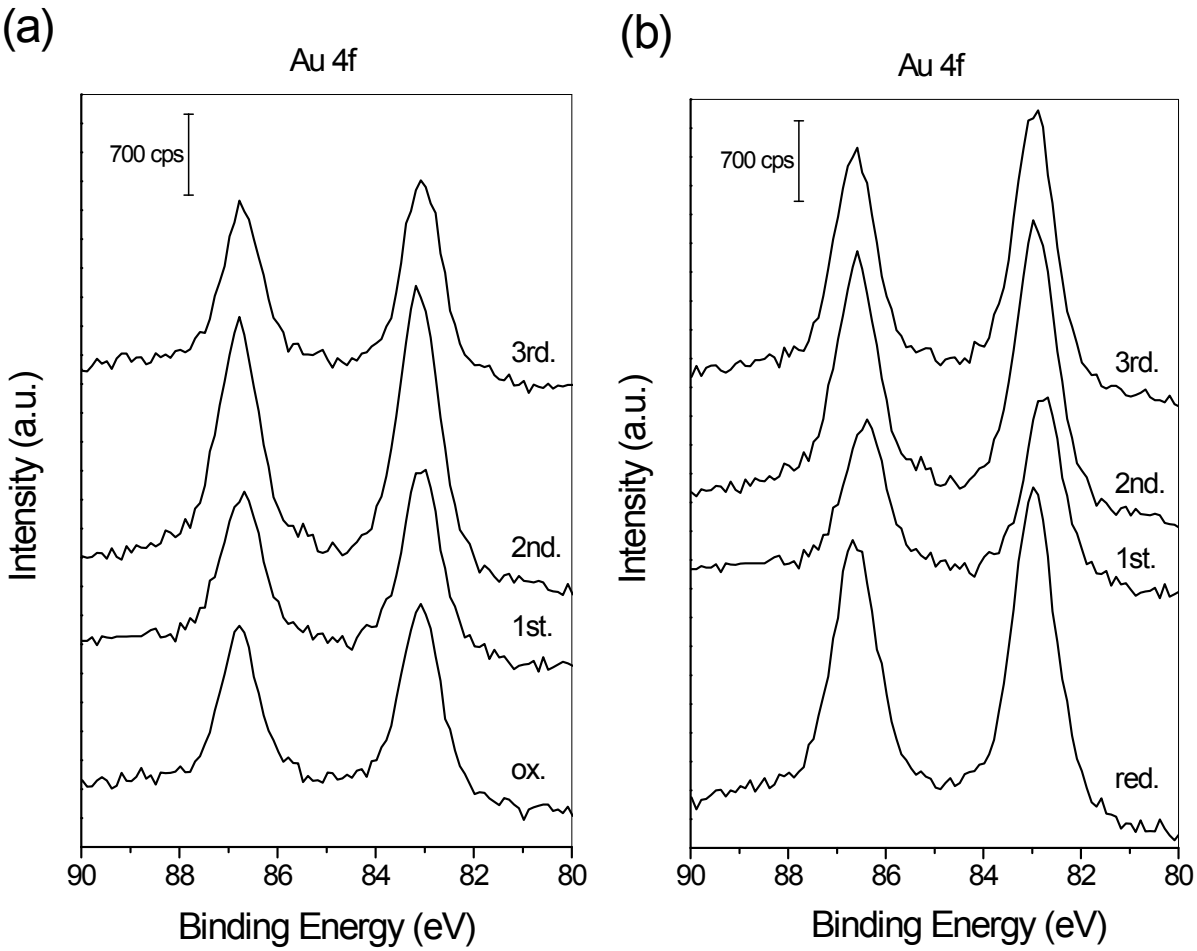

Figure S3. X-ray photoelectron spectra of the AuPd/TiO_2 materials in the Au4f region measured after the indicated CO oxidation temperature ramps: (a) oxidized samples and (b) reduced samples.

Besides surface composition, electronic states of metal nanoparticles can be evaluated from binding energy values (Table S1 and Figure S4a) in XPS data. In all bimetallic catalysts, the Au $4f_{7/2}$ peak was observed at ca. 83.0 eV, which is lower than the value expected for bulk Au, 84.0 eV. This shift can be attributed to a charge transfer from Pd to Au and is indicative of alloy formation.[2,3]

We have followed the evolution of total metal content of the catalysts after each temperature ramp. In the beginning of the experiment, oxidized catalyst has a much smaller total metal content (1.9% wt.) than reduced catalyst (5.0% wt.) (Table S2), indicating a considerable difference in metal dispersion between samples. Metal content of the oxidized catalyst remains nearly stable through the heating ramps, while that of the reduced catalyst markedly decreased (~40%) from the as prepared catalyst to the end of the third heating ramp. This is an evidence of nanoparticles aggregation in the reduced catalyst, lowering the dispersion of metal.

Table S1. XPS element energies and peak widths.

	Au $4f_{7/2}$ (eV)	FWHM (eV)	Pd^0 $3d_{5/2}$ (eV)	FWHM (eV)	Pd^{2+} $3d_{5/2}$ (eV)	FWHM (eV)
ox. as prep.	83.0 ± 0.1	1.07 ± 0.06	334.2 ± 0.1	1.31 ± 0.04	336.2 ± 0.1	1.5 ± 0.2
ox. 1st	83.2 ± 0.2	1.06 ± 0.03	334.5 ± 0.2	1.28 ± 0.03	336.4 ± 0.2	1.6 ± 0.2
ox. 2nd	83.09 ± 0.04	1.07 ± 0.04	334.38 ± 0.07	1.36 ± 0.02	336.32 ± 0.04	1.6 ± 0.1
ox. 3rd	83.05 ± 0.03	1.06 ± 0.04	334.35 ± 0.09	1.29 ± 0.04	336.30 ± 0.02	1.58 ± 0.07
red. as prep.	83.01 ± 0.04	1.14 ± 0.03	334.41 ± 0.04	1.32 ± 0.02	335.86 ± 0.03	2.8 ± 0.1
red. 1st	83.13 ± 0.06	1.14 ± 0.04	334.28 ± 0.09	1.15 ± 0.04	335.9 ± 0.2	3.04 ± 0.03
red. 2nd	83.0 ± 0.1	1.09 ± 0.03	334.3 ± 0.1	1.10 ± 0.06	335.9 ± 0.3	2.6 ± 0.3
red. 3rd	83.17 ± 0.02	1.09 ± 0.02	334.39 ± 0.05	1.05 ± 0.03	336.04 ± 0.05	2.4 ± 0.2

Table S2. Quantification of XPS data.

	Au (%wt.)	Pd^0 (%wt.)	Pd^{2+} (%wt.)	total metal (%wt.)
ox. as prep.	1.19 ± 0.09	0.23 ± 0,04	0.5 ± 0.2	1.9 ± 0.3
ox. 1st	1.04 ± 0.05	0.32 ± 0.03	0.42 ± 0.05	1.77 ± 0.03
ox. 2nd	1.01 ± 0.02	0.31 ± 0.03	0.41 ± 0.06	1.7 ± 0.1
ox. 3rd	1.18 ± 0.08	0.32 ± 0.06	0.5 ± 0.1	2.0 ± 0.2
red. as prep.	3.2 ± 0.1	1.1 ± 0.2	0.66 ± 0.03	5.0 ± 0.3
red. 1st	1.9 ± 0.1	0.53 ± 0.09	0.67 ± 0.05	3.2 ± 0.2
red. 2nd	1.7 ± 0.2	0.37 ± 0.06	0.6 ± 0.1	2.7 ± 0.3
red. 3rd	1.76 ± 0.09	0.39 ± 0.06	0.62 ± 0.03	2.8 ± 0.2

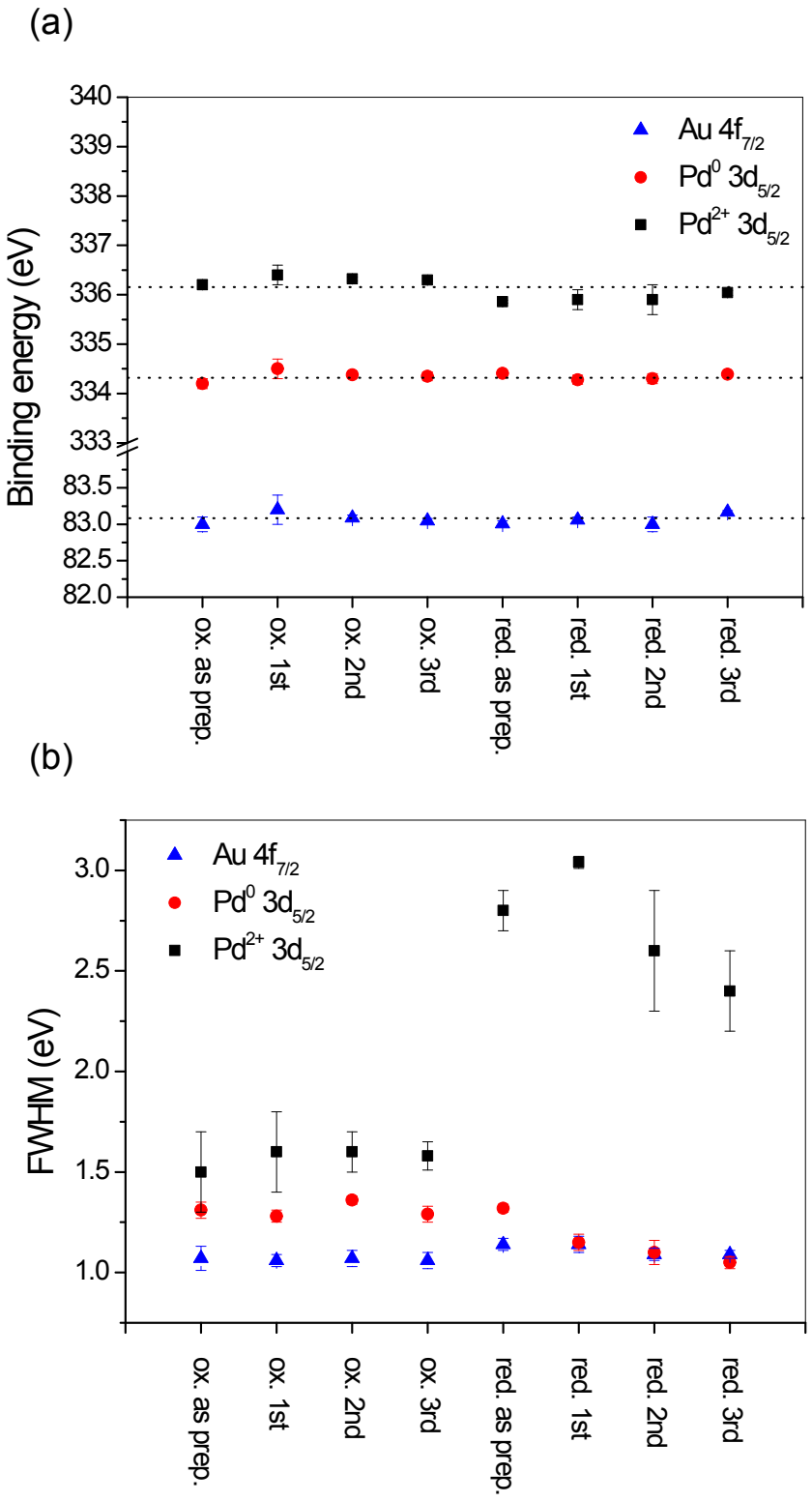

Figure S4. (a) Binding energies and (b) full width half maxima of Au $4f_{7/2}$ and Pd $3d_{5/2}$ elemental peaks measured after the indicated CO oxidation temperature ramps. Dotted lines in (a) are drawn to guide the eyes.

X-Ray Diffraction

XRD measurements of as prepared catalysts allowed the identification of crystalline phases present in each material. Characteristic peaks of anatase TiO_2 support dominate X-ray diffractograms of both oxidized and reduced catalysts in Figure S5.

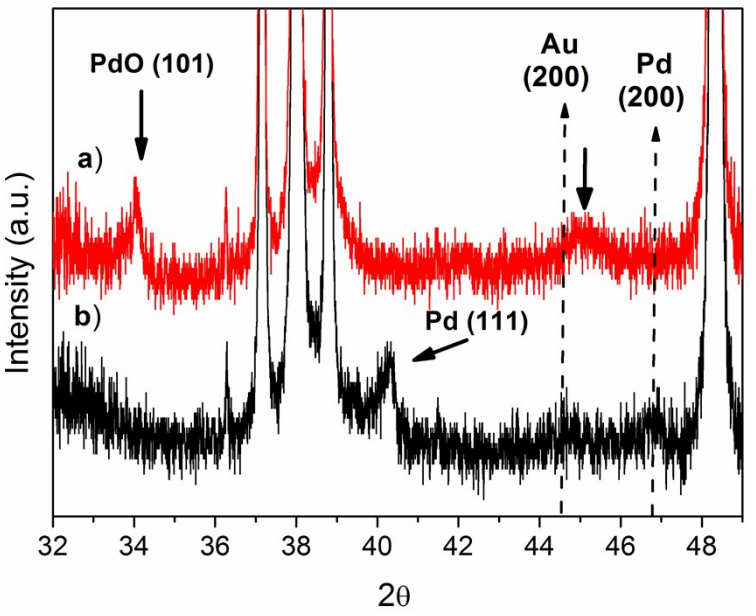

Figure S5. X-ray diffraction patterns of oxidized (red) and reduced (black) catalysts. Apart from the dominant anatase TiO_2 support reflections, broad reflections from metallic nanoparticles are present for both materials.

Oxidized material shows a PdO (101) peak and a broad peak at 2θ ~45°, which may be considered the Au (200) reflection broadened by the insertion of a few Pd atoms in the gold lattice, forming an AuPd nano alloy. The expected (111) peak of this alloy fcc structure is hidden

by the (103), (004) and (112) TiO_2 peaks in the 37°-39° range. Lee *et al.*[2] already showed the formation of separated PdO and AuPd alloy phases in a 1:3 AuPd/C catalyst by its thermal treatment (200 °C) under air. The observed segregation of PdO crystallites from the mixture of 1:1 AuPd precursors results in the formation of Au rich AuPd nanoparticles.

The reduced material resulted in a different crystalline structure. Figure S5 shows a peak at 2θ = 40.3°, which is attribute to Pd (111) peak of an almost pure metallic Pd phase. The position of the noise hidden Pd (200) peak is indicated, along with that of Au (200) peak. This result suggests the presence of an Au rich metallic phase, along with the Pd rich phase, with the expected Au (111) peak (2θ =38.3°) hidden by the TiO_2 peaks. PdO (111) peak is absent in the reduced material. Segregation of two populations of gold- and palladium-rich AuPd alloyed particles was previously demonstrated by Xu *et al.*[5] after the thermal treatment of catalyst samples in reducing atmosphere. Based on our XRD data, the entire population of the oxidized catalyst particles can be described as a mixture of PdO and Au rich AuPd alloyed nanoparticles deposited on TiO_2. By contrast, the population of reduced catalyst particles can be described as a mixture of metallic Au- and Pd-rich nanoparticles deposited on TiO_2.

---

2 - S.-Y Lee, N. Jung, J. Cho, H.-Y. Park, J. Ryu, I. Jang, H.-J. Kim, E. Cho, Y.-H Park, H.C. Ham, J.H. Jang, S.J. Yoo, *ACS Catal.* **2014**, *4*, 2402–2408.

5 - J. Xu, T. White, P. Li, C. He, J. Yu, W. Yuan, Y.-F. Han, *J. Am. Chem. Soc.* **2010**, *132*, 10398–10406.

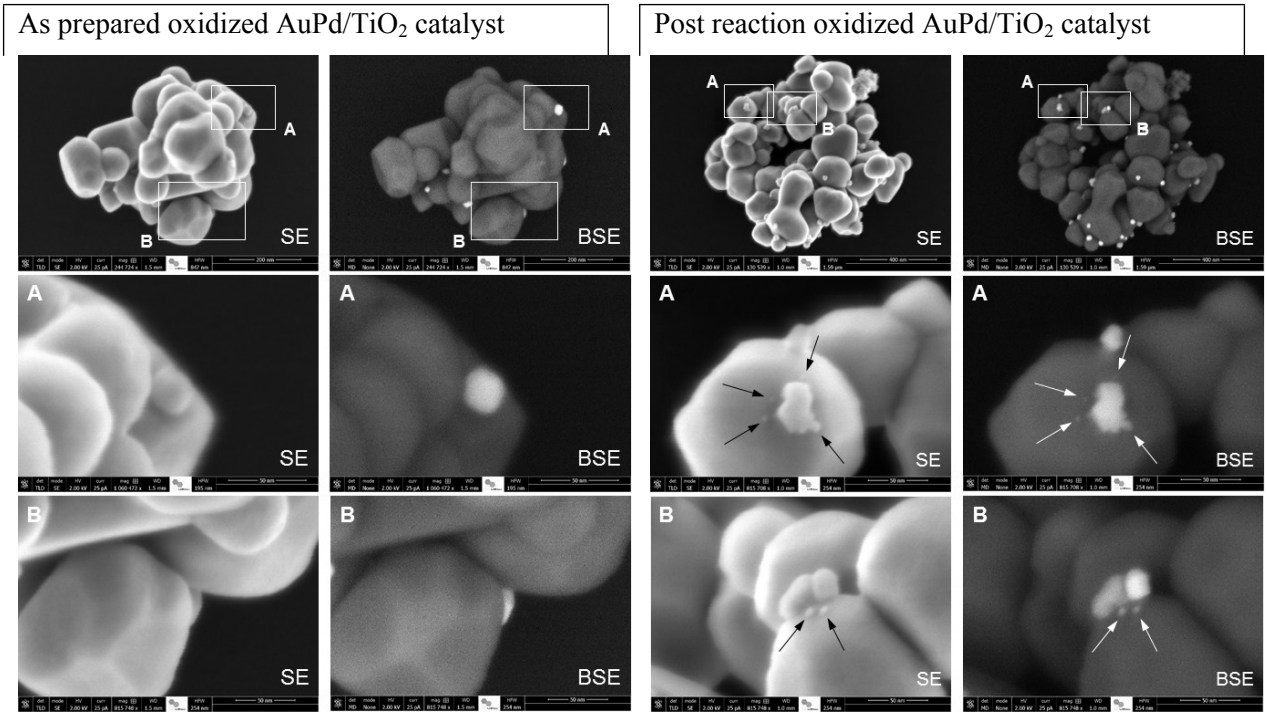

Figure S6. Secondary electron (SE) and backscattered electron (BSE) images of the AuPd/TiO_2 oxidized catalysts as prepared (left) and after CO oxidation temperature ramps (right). The areas marked by A and B rectangles in the top images of both catalysts are shown in the higher magnification images A and B bellow. The appearance of a new population of small particles in the post reaction catalyst is seen indicated by the arrows.

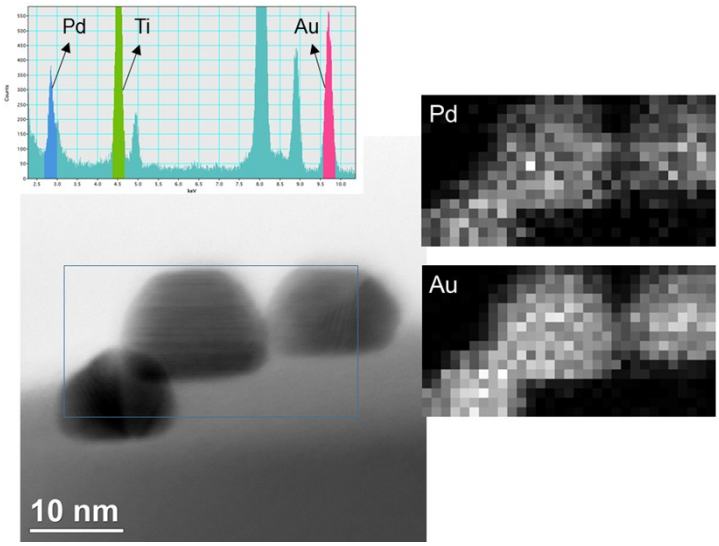

Figure S7. BF-STEM image of the as-prepared AuPd/TiO_2-oxidized catalyst. The XEDS-SI elemental maps shows a uniform elemental distribution throughout the particles.

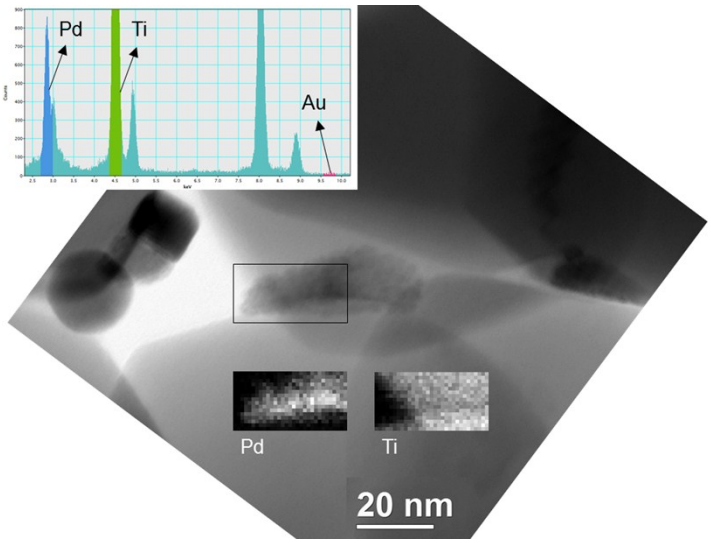

Figure S8. BF-STEM image of the as-prepared AuPd/TiO_2-oxidized catalyst showing an irregularly shaped particle deposited on TiO_2. This irregularly shaped particle appears as a Pd-only domain (see inserted XEDS spectrum) deposited on Ti in the XEDS-SI elemental maps.

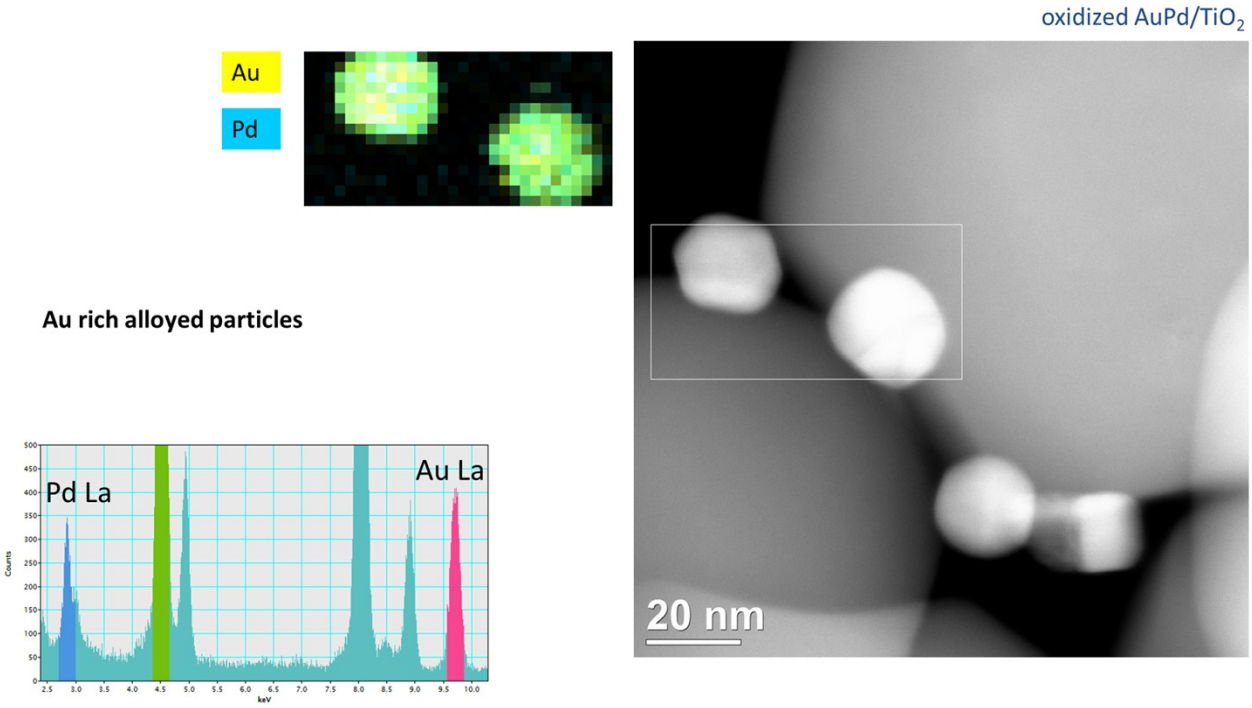

Figure S9. High-angle annular dark field (HAADF) STEM image of the as-prepared $AuPd/TiO_2$ oxidized catalyst and XEDS-SI compositional map from the area marked by a white rectangle. Analysis of the XED spectrum measured from this area reveal that these are Au rich AuPd alloyed particles: 62/38 XEDS counts proportion.

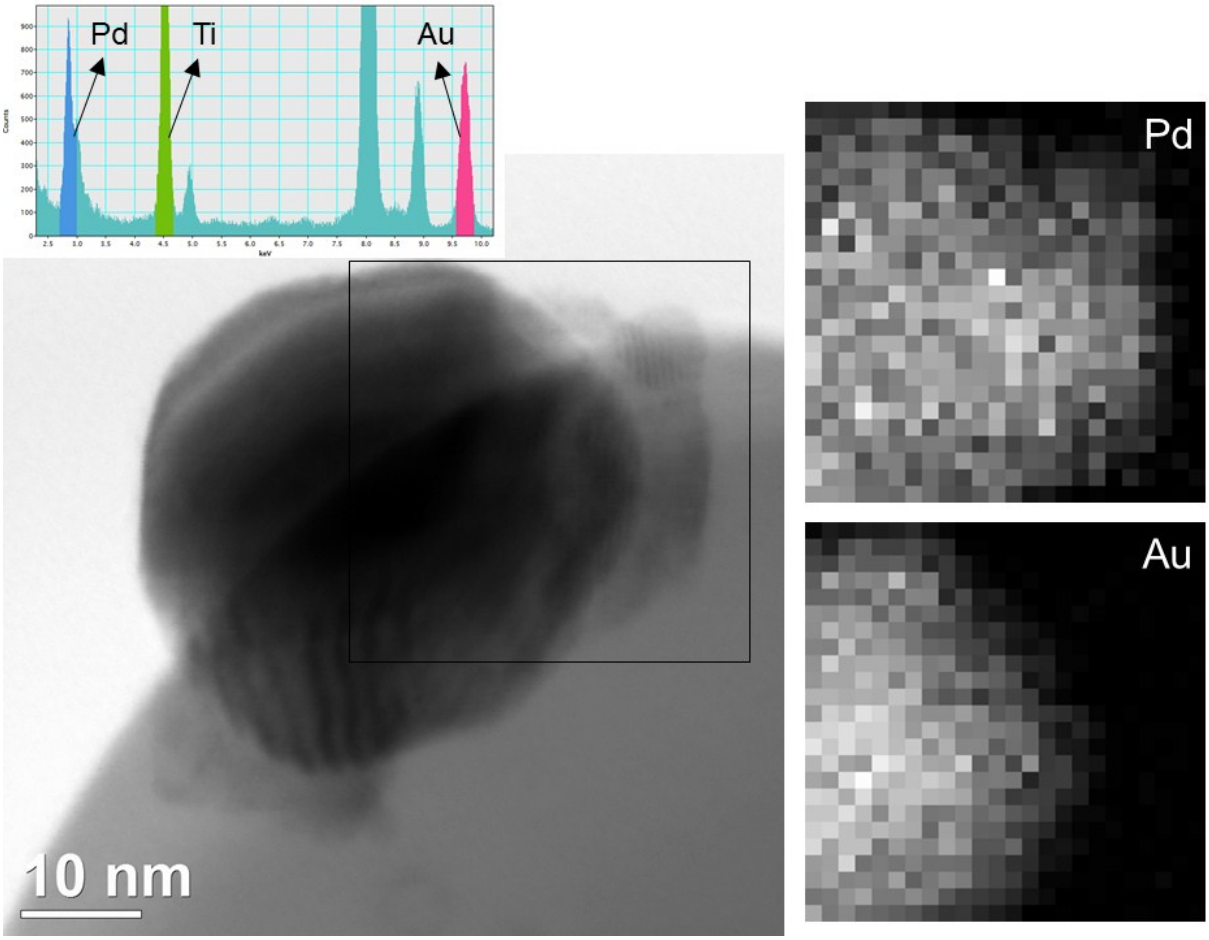

Figure S10. BF-STEM image of the AuPd/TiO_2-oxidized catalyst after the CO oxidation reaction showing an hemispherical particle deposited on TiO_2. XEDS-SI compositional maps from the squared area in the image discloses the AuPd alloyed core and Pd-only shell structure of the particle.

Reduced $AuPd/TiO_2$ catalyst

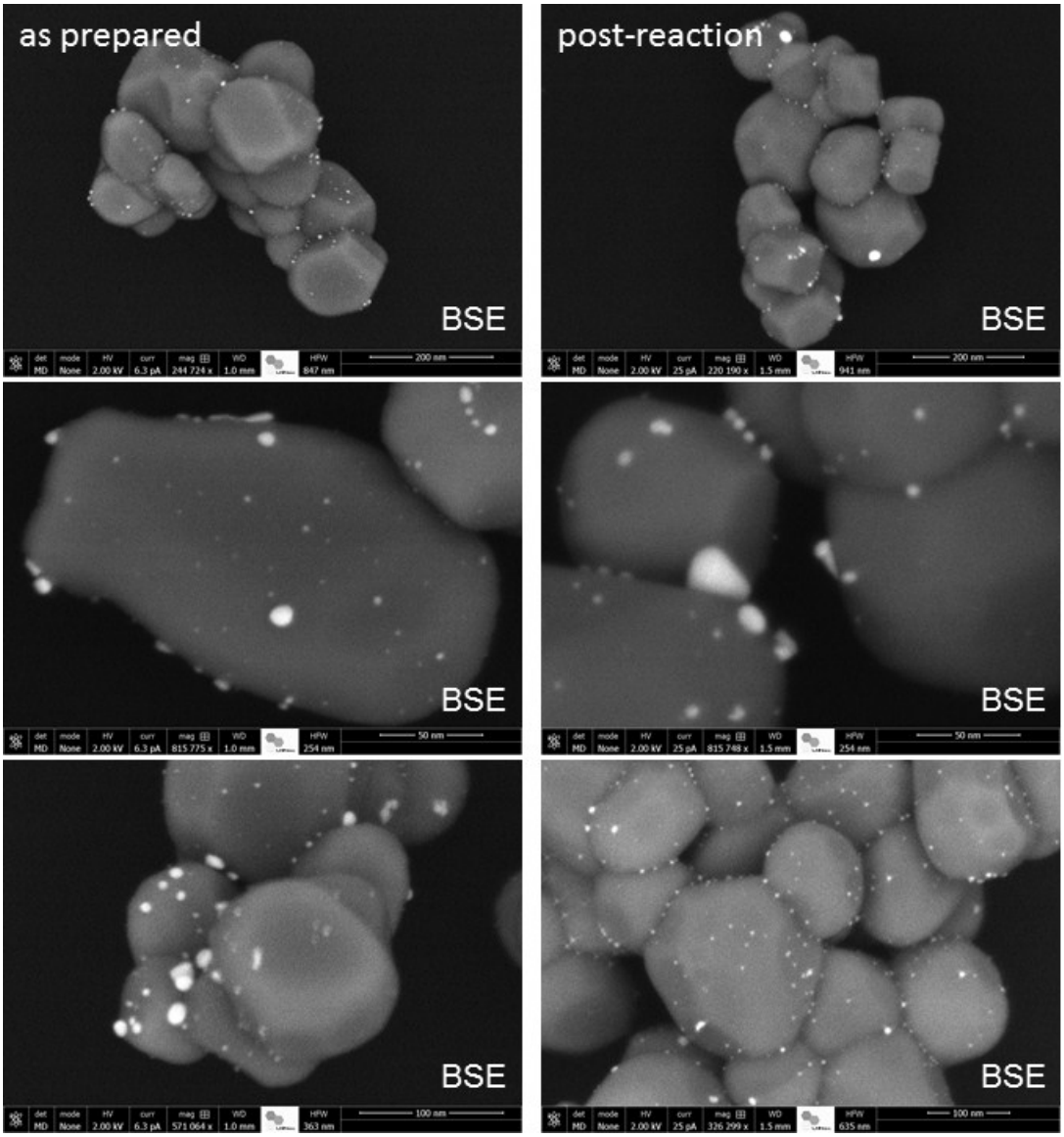

Figure S11. Backscattered electron (BSE) images of the $AuPd/TiO_2$ reduced catalysts as prepared (left) and after CO oxidation temperature ramps (right). Particles appear uniformly rounded and bright in the images for both catalysts, with no obvious morphological change after the reaction.

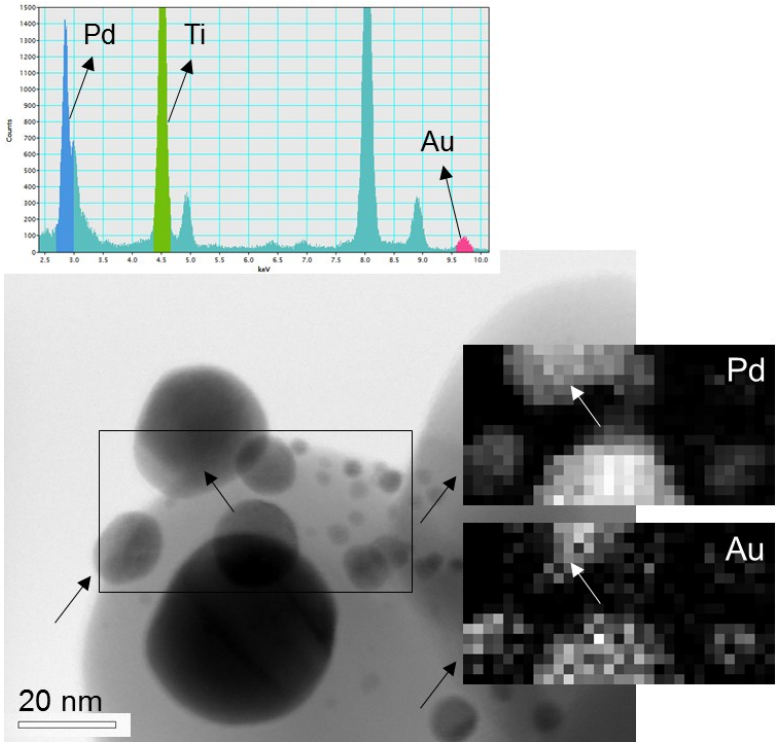

Figure S12. BF-STEM image of the as-prepared AuPd/TiO_2 reduced catalyst. The XEDS-SI elemental maps show the segregation of the Au domains to the surface of alloyed particles, indicated by arrows.

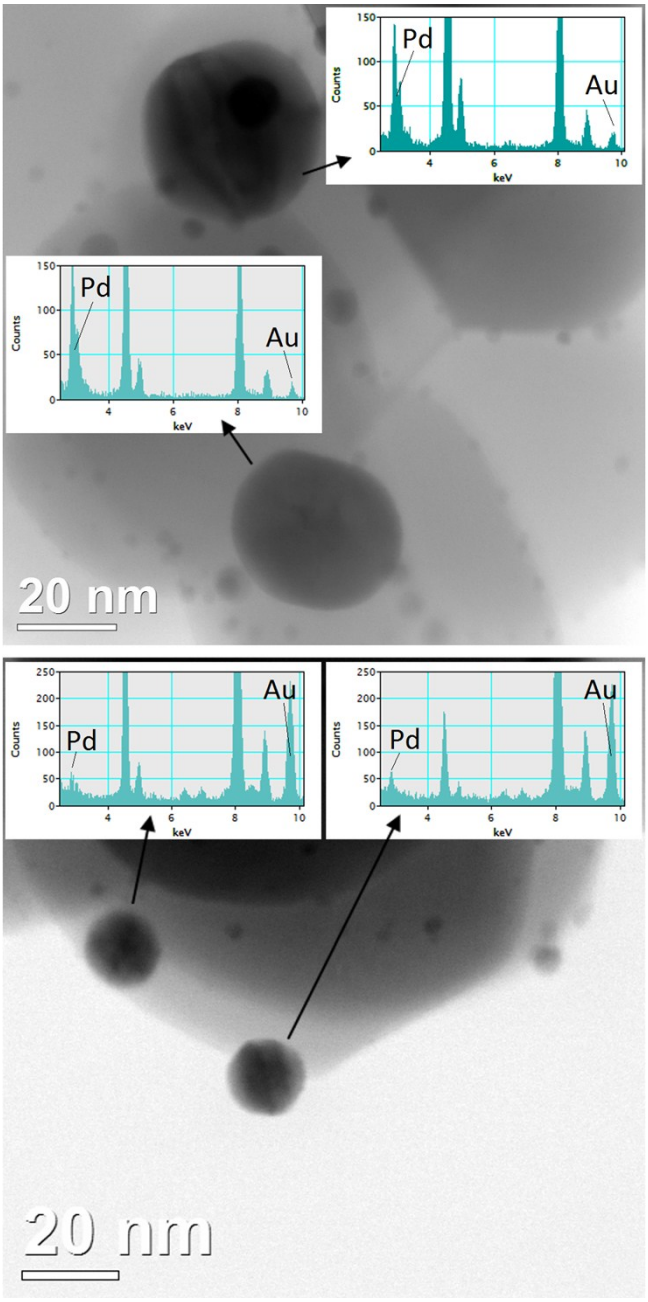

Figure S13. Bright-field (BF) STEM images of the as-prepared AuPd/TiO_2 reduced catalyst. Pd Lα (2.84 keV) and Au Lα (9.71 keV) peaks are indicated in each XED spectra, showing the coexistence of separated very rich Pd (top image) and Au (bottom image) particles in this material.

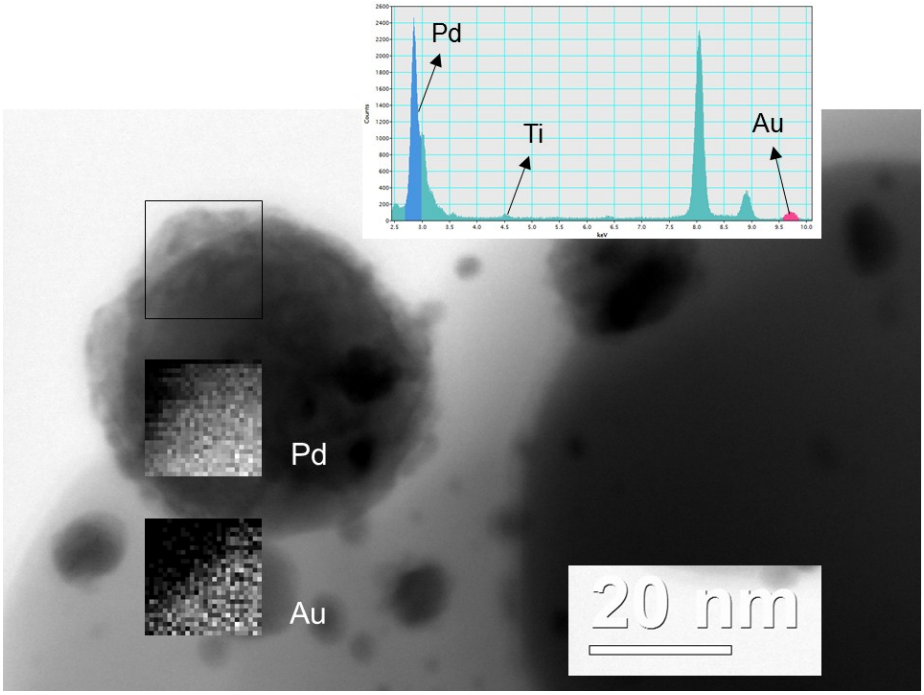

Figure S14. BF-STEM image of the AuPd/TiO_2 reduced catalyst after the CO oxidation reaction. XEDS-SI elemental maps reveal an AuPd alloyed particle with a separated PdO domain on the particle surface.